










CORRESPONDENCE

Open Access



Effect of pure (ligand-free) nanoparticles of magnetite in sodium chloride matrix on hematological indicators, blood gases, electrolytes and serum iron

Stanislav Ye. Lytvyn^{1*} , Elena M. Vazhnichaya² , Daniela E. Manno³ , Yurii A. Kurapov¹ , Lucio Calcagnile³ , Rosaria Rinaldi³ , Giorgio Giuseppe Carbone³ , Oleksandr V. Semaka²  and Yana V. Nedostup⁴ 

Abstract

One of the physical methods for obtaining magnetite nanoparticles (NPs) is electron beam physical vapor deposition (EB PVD), which requires complex equipment, but allows obtaining a significant amount of pure (ligand-free) NPs. The biomedical application of such NPs is less studied than materials from other synthesis methods. The objective is to study the effect of pure magnetite NPs in the NaCl matrix obtained by EB PVD on hematological indicators, gases, electrolytes and parameters of iron metabolism in the blood of intact animals. The physical characteristics of NPs were studied using high-resolution transmission electron microscopy, scanning transmission electron microscopy, energy-dispersive X-ray spectroscopy mapping, electron energy-loss spectroscopy, selected area electron diffraction and fast Fourier transform. In vivo experiments were conducted on albino male rats, which were injected with solution of magnetite-sodium chloride NPs (1.35 mg Fe/kg). After 3 and 72 h, hematological parameters, blood gases, electrolytes, and serum iron were determined. The synthesized NPs had an average size of 11 nm. They were identified as magnetite, where polycrystals and single crystals were present. The absence of contamination in crystal boundaries, clear orientation and orderliness of atoms in crystals were established. The administration of NPs in the sodium chloride matrix to animals was characterized by a transient increase in the main indicators of red blood accompanied by an increase in the saturation of erythrocytes with hemoglobin and their mean volume after 3 h. It did not worsen blood gases and pH, but decreased blood Na⁺ content after 72 h. The investigated NPs caused changes in the parameters of serum iron characteristic to iron preparations, which after 3 h were smaller compared to the reference iron drug, and after 72 h—similar to it. More intense rapid effects on hematological parameters at lower serum iron indicate greater activity of the studied pure magnetite NPs obtained by EB PVD synthesis compared to the reference iron preparation.

Highlights

- Pure magnetite nanoparticles in the NaCl matrix were obtained by EB PVD.
- They were studied using high-resolution transmission electron microscopy.
- These nanoparticles had a size of 11 nm, clear orientation and orderliness of atoms in crystals.

*Correspondence:

Stanislav Ye. Lytvyn
lytvynse@hotmail.com

Full list of author information is available at the end of the article



© The Author(s) 2024. **Open Access** This article is licensed under a Creative Commons Attribution 4.0 International License, which permits use, sharing, adaptation, distribution and reproduction in any medium or format, as long as you give appropriate credit to the original author(s) and the source, provide a link to the Creative Commons licence, and indicate if changes were made. The images or other third party material in this article are included in the article's Creative Commons licence, unless indicated otherwise in a credit line to the material. If material is not included in the article's Creative Commons licence and your intended use is not permitted by statutory regulation or exceeds the permitted use, you will need to obtain permission directly from the copyright holder. To view a copy of this licence, visit <http://creativecommons.org/licenses/by/4.0/>.

- In healthy animals, they caused a transient increase in red blood indicators.
- They did not worsen blood gases and pH, but decreased Na⁺ content in the blood.
- The nanoparticles caused changes in the serum iron typical to iron preparations.
- These changes were not toxic and lasting due to compensatory reactions.

Keywords Ligand-free magnetite nanoparticles, High-resolution transmission electron microscopy, Erythrocyte, Blood gas, Electrolyte, Serum iron, Total iron-binding capacity, Transferrin saturation

Introduction

Due to their unique properties, nanoparticles (NPs) based on metals and their oxides attract the attention of researchers [1]. Among them, NPs of magnetite, or iron oxide II, III (Fe₃O₄) are one of the most famous. They are characterized by superparamagnetic properties, biocompatibility and the presence of iron, which can be included in metabolic processes [2]. Natural magnetite NPs are present in biological systems and participate in physiological processes [3]. Artificial magnetite NPs are obtained by numerous methods of synthesis: chemical, physical, or methods of green synthesis [4]. The problem in the chemical synthesis is that post treatments are usually needed to remove the residual ligands to clean the surface of NPs. These post treatments could alter the surface structure of the prepared NPs and deteriorate the catalytic performance or biomedical activity [5]. Therefore, it is interesting to directly prepare NPs with ligand-free properties. One of the physical methods which allows to obtain a significant amount of pure (ligand-free) metal/metal oxide NPs, including magnetite NPs, is the electron beam technology in vacuum [6].

A surface of magnetite NPs can be modified by coating with various organic and inorganic compounds for stabilization in certain environments, ensuring the binding of other molecules or extending the half-life [7]. This fully applies to ligand-free magnetite NPs and widens the prospects for their use [8].

The biomedical application of magnetite NPs is based on their high biocompatibility, ability to overcome biological membranes, appropriate surface architecture, and easy binding to ligands [9]. On their basis, drugs for contrast in magnetic resonance imaging [10], remedies for the treatment of cancer through hyperthermia [11] and iron deficiency in patients with chronic renal failure and hemodialysis [12] were created and introduced into the clinic. Magnetic NPs are also being investigated as platforms for drug delivery, tools for regenerative medicine and laboratory diagnostics [13, 14]. They can be used to monitor the state of the environment and neutralize its pollutants [15]. They have prospects of use for the intensification of biotechnological processes, for example, in the production of antibiotics or biological drugs [16].

It is known that the pharmacokinetics of magnetite NPs is determined by their size and coating and, for the most part, is characterized by rapid distribution and elimination [17]. This property allowed us to use magnetite NPs to quickly obtain an effect in emergency conditions, specifically, in post-hemorrhagic syndrome, when magnetite NPs functionalized with sodium chloride (NaCl), polyvinylpyrrolidone polymer and (or) the synthetic antioxidant ethylmethylhydroxypyridine succinate already through 3 h improved hematological parameters and critical condition indicators [18, 19]. However, in order to more accurately determine their therapeutic effectiveness, it is necessary to study the effect of these NPs not only under the conditions of experimental pathology, but also in intact animals. Other reason to investigation of magnetite NPs engineered by the electron beam technology is their more rare use for biomedical application than nanomaterials from other synthesis methods and minimal information about features of pharmacological effects. This opinion determined the objective: to study the effect of pure magnetite NPs in the NaCl matrix obtained by the method of electron beam physical vapor deposition (EB PVD) on hematological parameters, gases, electrolytes and iron metabolism parameters in the blood of intact animals.

Materials and methods

Materials

Magnetite NPs in a sodium chloride matrix were obtained by electron beam technology in vacuum in Laboratory of Electron Beam Nanotechnology of Inorganic Materials for Medicine of E.O. Paton Electric Welding Institute of the National Academy of Sciences of Ukraine [18]. That is, a thick film of Fe-NaCl condensate was obtained by the EB PVD of iron and NaCl with the condensation of a mixed vapor stream on a stationary substrate in vacuum. When maintaining a sufficiently low iron concentration in the NaCl matrix, pure (ligand-free) magnetite NPs are formed.

For experiments on animals, the solution of 10 mg of powdered pulverized condensate (20 wt% Fe-NaCl with NPs Fe₃O₄) was prepared in 10 ml of bidistilled water at 56 °C and constant shaking for 2 h. Ferrum Lek injection

solution (ferric hydroxide (III) polyisomaltosate (Pharmaceutical Company "Lek", Slovenia) was used as a reference iron preparation. Sterile isotonic NaCl solution (Halychpharm ATVT, Ukraine) was used for administration to control rats. The content of iron in blood plasma and the total iron-binding capacity (TIBC) were determined using standard sets of reagents of LLC NVP "Filisit-Diagnostika" (Ukraine). Blood samples were collected in BD Vacutainer tubes without anticoagulant or with K₂-EDTA (Chengdu Rich Science Industry Co., Ltd, China).

High-resolution transmission electron microscopy (HR TEM) assay

High-resolution transmission electron microscopy (HRTEM) observations were carried out using a JEM-ARM200F NEOARM electron microscope (JEOL, Japan) at 200 kV at the University of Salento (Lecce, Italy). The microscope enables remarkable brilliance and spatial coherence due to the cold cathode field emission electron source (C-FEG), achieves 68 pm resolutions by means of a CETCOR/ASCOR double spherical aberration corrector. The images were recorded by a Gatan Rio16 complementary semiconductor metal-oxide-semiconductor (CMOS) digital camera with a resolution of 16 MP (4,096×4,096). STEM (scanning transmission electron microscopy) images of the material were acquired in STEM-SI mode to correlate morphological and chemical features. Briefly, the incoming electron beam is focused on a succession of image points (from a few nanometers to near-atomic size), from which, a complete EDS (energy-dispersive X-ray spectrum) and/or EELS (electron energy-loss spectrum) were also stored. In this way, conventional STEM imaging has been supplemented with spectrum imaging (SI). The results were processed with DigitalMicrograph software v.3.53.4137.0 (Gatan Inc, USA), which allows the interpretation of SAED (Selected Area Electron Diffraction) patterns and fast Fourier transform (FFT) to identify the synthesized phases.

In vivo experiments design

In vivo experiments were conducted on 35 albino male Wistar rats. The animals were obtained from the Experimental Veterinary Clinic of the Poltava State Medical University (Poltava, Ukraine). Rats with a body weight of 183–221 g were used in the experiments. They were kept in polycarbonate cages measuring 660×370×140 mm with lids made of galvanized steel wire and glass water bottles. In the room for keeping animals during the experiment, the following conditions were maintained: temperature +20–24 °C, air humidity 30–70%, lighting cycle—12 h light / 12 h dark. Rats were randomized,

labeled with fucorcin solution and divided into groups (intact, control, reference, and experimental). The group of intact animals (without any experimental intervention) was combined for both periods of the study (3 and 72 h after the start of the experiment). The conducting of experiments did not raise any objections from the Commission on Ethical Issues and Bioethics of the Poltava State Medical University (protocol 197 from Sept 23, 2021).

The magnetite NPs solution in a dose of 5 mg condensate/kg (1.35 mg Fe/kg) was administered to rats intraperitoneally, which was an average of 1 ml of solution for an animal weighing 200 g. The iron preparation for parenteral administration Ferrum Lek was administered similarly in a dose of 1.25 mg Fe/kg body weight. Animals of the control group received an intraperitoneal injection of 1 ml of isotonic sodium chloride solution.

The animals were removed from the experiment 3 and 72 h after the administration of the studied agents by means of terminal blood loss under ether anesthesia (3–4 ml/kg) [20]. In the blood obtained during euthanasia from the left ventricle of the heart and stabilized with K₂-EDTA, hematological indicators, blood gases and electrolytes were determined. The rest of the blood sample without stabilizer was used to obtain blood serum by the standard procedure.

Determination of hematological indicators

Blood samples were studied for total erythrocyte count (RBC), hematocrit (Hct), total hemoglobin (Hb), mean cell volume (MCV), mean erythrocyte hemoglobin concentration (MCHC), mean erythrocyte hemoglobin count (MCH) and anisocytosis index (width of red blood cell distribution) (RDW). These indicators were studied using the hematological analyzer MicroCC-20Plus Vet (High Technology Inc., USA), programmed for the blood parameters of albino rats [21], according to the manufacturer's instructions.

Since the content of reticulocytes (Rt) serves as an indicator of the regenerative reaction of the bone marrow, the count of these cells in the circulating blood was determined. For this purpose, the classic method of supravital staining with methylene blue was used, during which RNA-containing structures are revealed in the form of a granular-reticulate substance [22]. Stained smears were examined with a×100 objective on a MICROmed XS-3320 microscope (China).

Blood gases and electrolytes analysis

In blood samples from the left ventricle, the partial pressure of carbon dioxide (pCO₂) and oxygen (pO₂), hemoglobin oxygen saturation (saO₂), volume concentration of oxygen (ctO₂), hydrogen index (pH) and content of

bicarbonate (HCO_3^-), sodium (Na^+), potassium (K^+), and calcium (Ca^{2+}) were investigated using a portable analyzer of electrolytes and blood gases OPTI CCA-TS (OPTI Medical Systems Inc., USA) with an E-Ca cassette [23].

Assay for the serum iron, total iron-binding capacity and saturation of transferrin with iron

The iron content in blood serum was studied using the reaction with ferrozine [24]. The principle of the method is that iron is released from the iron-binding peptides of blood serum and reduced due to the action of guanidine and hydroxylamine. The sodium salt of 3-(2-pyridyl)-5,6-bis(4-sulfophenyl)-1,2,4-triazine (ferrozine) gives a purple complex with Fe^{2+} ions. The optical density of the test solution is proportional to the concentration of iron in the sample.

To saturate transferrin, the serum is treated with an excess amount of Fe^{3+} ions. The solution is freed from unbound iron ions using magnesium carbonate. By determining the concentration of iron in saturated serum, its TIBC is found [25]. The transferrin saturation coefficient is found as the ratio of the iron content in the serum to the TIBC expressed in %. All determinations and calculations were carried out in full accordance with the instructions of the manufacturer of diagnostic kits. Measurements were performed on a spectrophotometer Ulab-102 (Ulab COMPANY: LLC Chemlaborektiv, China).

Statistical analysis

The data from the in vivo experiments was statistically processed using standard computer programs of the Statistica for Windows 8.0 package. The mean (M) and its standard error (SEM) were calculated, and the probability of a difference between groups was estimated using one-way analysis of variance (ANOVA) with Tukey's a posteriori test.

Results

HRTEM results

Pure (ligand-free) 20 wt% Fe-NaCl condensates obtained by the EB PVD method were studied by TEM methodology. Figure 1 presents typical results of elemental composition (EDS spectrum in picture 1A) and structural phase (SAED pattern in picture 1B).

The obtained EDS spectrum showed the presence of a large amount of bound oxygen in the condensate and small amount of Na and Cl. A non-standardized quantitative analysis was performed on this EDS spectrum to obtain the concentration of the majority and minority elements in the sample. The results are shown in Table 1 and report the mass fractions (wt%) and weight

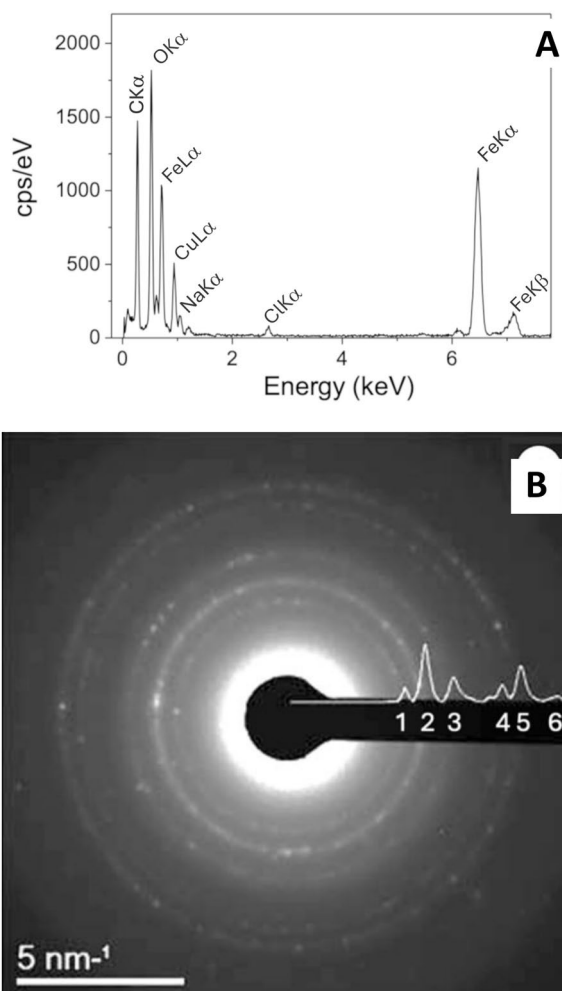


Fig. 1 EDS spectrum (A) and SAED pattern (B) EB PVD condensate 20 wt% Fe-NaCl

percentages (at %) of the identified elements. The presence of a small amount of Na and Cl is explained by the presence of NaCl, a residue from the synthesis of the material, and the high localization of the EDS analysis.

Table 1 shows the elemental composition of the condensate calculated from the K-lines of the specified elements. The presence of a small amount of NaCl is explained by the high locality of the EDS analysis.

The SAED pattern in Fig. 1B made it possible to determine the polycrystalline nature of the material. The pattern was carefully analyzed and the intensity profile obtained from the stereoscopic projection is shown above the figure; the peaks were labeled with numbers that, as summarized in Table 2, correspond to the crystallographic planes of the Fe_3O_4 magnetite phase (AMCS database <https://rruff.geo.arizona.edu/AMS/amcsd.php>). The caption of Table 2 states 'The obtained parameters correspond to the Fe_3O_4 magnetite phase.'

Table 1 Elemental composition EB PVD condensate 20 wt% Fe-NaCl from EDS spectrum (Fig. 1A)

Element	Shell	Signal, Counts	Comp., at%	Comp., Wt%	k-Factor, 1/Si	Det Corr
O	K	12960 ± 120	51.1 ± 0.4	23.49 ± 0.19	1.290	0.78
Na	K	740 ± 30	1.67 ± 0.07	1.10 ± 0.05	1.064	0.96
Cl	K	480 ± 30	0.74 ± 0.04	0.75 ± 0.04	1.117	0.96
Fe	K	35,130 ± 190	46.50 ± 0.12	74.65 ± 0.19	1.512	1.0

Table 2 Interplanar spacings corresponding to the rings numbered in SAED pattern (Fig. 1B)

# peaks on Fig. 1B	d, nm	Hkl	I
1	0.297	220	30
2	0.253	311	100
3	0.210	400	20
4	0.161	511	25
5	0.148	440	41
6	0.128	533	9

The obtained parameters correspond to the Fe₃O₄ magnetite phase (American Mineralogist Crystal Structure Database (AMCS) <https://ruff.geo.arizona.edu/AMS/amcsd.php>)

Figure 2 shows the EELS spectra obtained on our iron oxide nanoparticles, picture A reports the spectral region 450–900 eV, pictures b and c – the O K-edge and Fe L-edge spectral components plotted together with reference spectra for Fe₃O₄ (red line) as results in <https://eelsdb.eu> database [26].

The O K edge (Fig. 2B) is composed of a pre-peak and a broad edge at higher energy. The pre-peak results from the hybridization of Fe 3d and O 2p and its intensity depend on iron valence state. The broad edge is correlated to density of states (DOS) from oxygen p levels hybridized with iron 4 s and 4p states. In our case, an asymmetric O K with a shoulder located a 530 eV on the high-energy side of the pre-peak was observed, as in the case of magnetite [27].

The L_{2,3} edge of Fe (Fig. 2C) shows an enlarged peak, these unusual structure is the result of the mixture of various iron sites [28] and of the more delocalized electronic structure of magnetite compared to most of other mixed iron oxides [29].

The resulting size distribution of NPs in the field of view of the TEM image (Fig. 3A) showed that the synthesized NPs are distributed according to the Gauss law with an average size of 11 nm and standard deviation of 5 nm (Fig. 3B).

EDS, EELS and SAED all confirm that the nanoparticles of iron oxide crystallize into the magnetite structural modification and conventional TEM microscopy show

that our sample is made by NPs having mean diameter of 11 nm. The STEM/HAADF image and EDS mapping (Fig. 4) give the particles morphology and the EDS mapping of iron (Fig. 4B), oxygen (Fig. 4C), sodium (Fig. 4D) and chlorine (Fig. 4E), they are (respectively) distributed in the area of location of the corresponding element: Fe + O, Na + Cl.

Further investigation of the TEM image (Fig. 5A) made it possible to distinguish the NPs according to the orientations of the single crystals (Fig. 5B) by fast Fourier transform (Fig. 5C), and in combination with the STEM image (Fig. 5D) to obtain the internal atomic structure of the NPs. The frequencies in Fig. 5C are arranged as in the SAED pattern and have been correspondingly indexed. Thus, the nanocrystals in Fig. 5B have the structure of magnetite. Further magnification (Fig. 5D) of one of the grains shows a lattice image from the Fe₃O₄ structure in the slightly misoriented (021) orientation as in the model obtained by VESA superimposed to the image.

A further magnification (Fig. 5D) of one of the grains shows an image of the Fe₃O₄ lattice, the grain results in the axis of the {1–10} zone of the magnetite structural change, and the simulation of the high-resolution image (detailed in the Supporting Information), as shown by the result superimposed on the experimental image and highlighted in yellow, matches the experimental image perfectly.

Hematological indicators

It was shown that the main indicators of red blood for the control group of animals with the administration of physiological NaCl solution did not differ from those of intact rats (Table 3). 3 h after administration of the reference iron preparation, RBC and Hct were at the control level, and Hb increased by 11% ($p < 0.02$) compared to it. Administration of the Fe₃O₄@NaCl solution at this period was characterized by an increase in not only Hb ($p < 0.005$), but also in RBC by 9% ($p < 0.05$) and Hct by 15% ($p < 0.001$) compared to control. The effect of NPs on RBC and Hct was more pronounced than the reference drug action ($p < 0.05$ and $p < 0.001$, respectively).

3 h after injection, Ferrum Lek caused an increase in erythrocyte indices MCH and MCHC ($p < 0.001$) versus

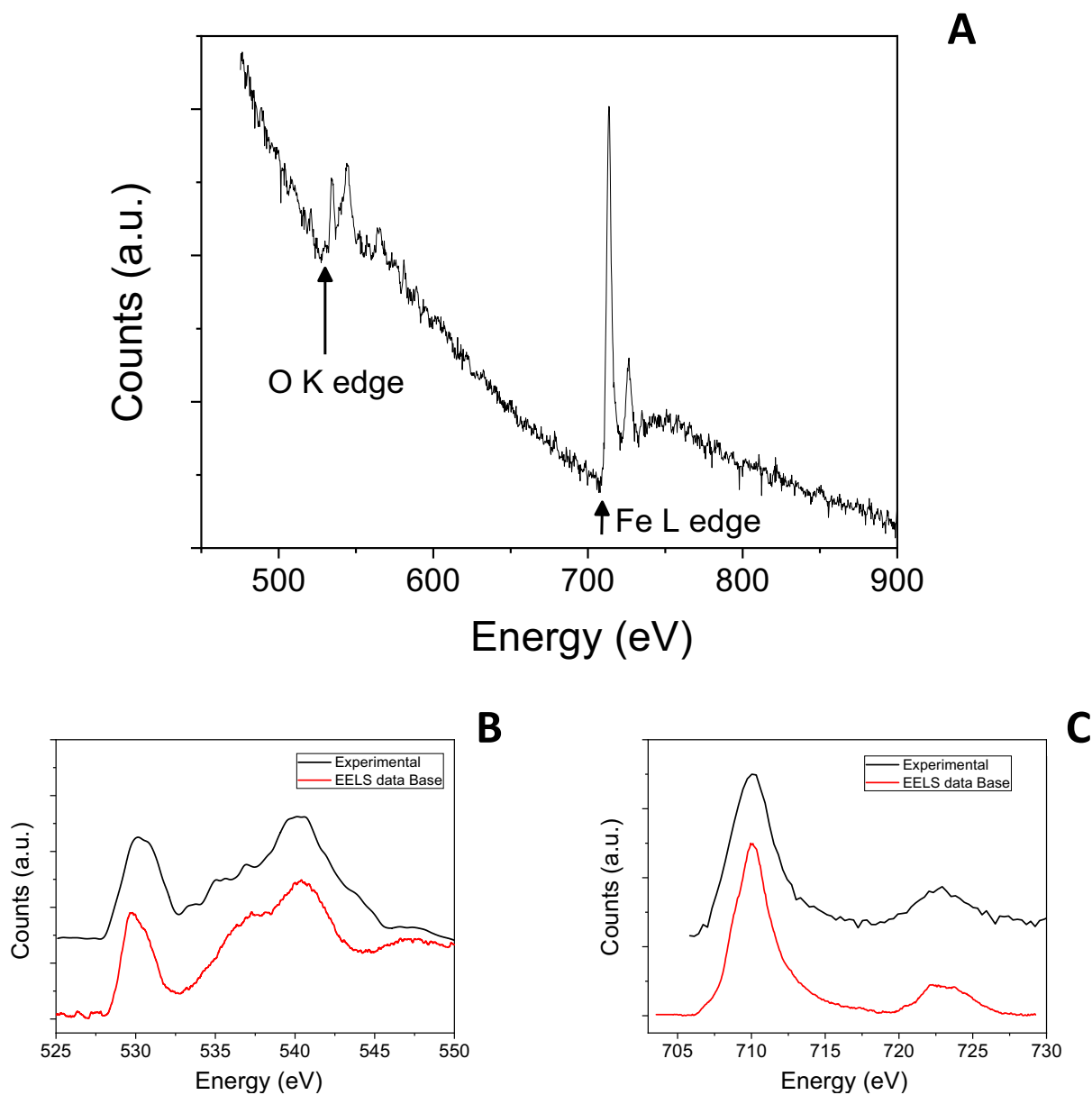


Fig. 2 EELS spectra obtained from EB PVD 20 wt% Fe-NaCl condensate. Picture **A** show the full spectra 450 and 900 eV. Picture **B** and **C** show the O K-edge and Fe L-edge spectral components plotted together with reference spectra for Fe_3O_4 , as results in <https://eelsdb.eu> database

control. The $\text{Fe}_3\text{O}_4@NaCl$ NPs in this period of observation contributed to an increase in MCV ($p < 0.05$) and MCH ($p < 0.02$), and these indicators were probably higher than those when using the reference iron preparation. The MCHC index in this group did not differ from the control, but was lower than when Ferrum Lek was administered ($p < 0.001$).

The blood of intact animals contained an average of 50.4% reticulocytes. The content of these cells in animals of the control group was the same. 3 h after the Ferrum Lek injection, it did not differ from the control.

In this period of observation, the content of Rt in rats with the NPs administration was also at the control level.

In the study after 72 h of the Ferrum Lek administration, values of RBC and Hct did not change as compared to intact and control groups (Table 4). At the same time, in these animals, Hb was increased ($p < 0.01$) compared to the control. 72 h after the administration of $\text{Fe}_3\text{O}_4@NaCl$ NPs, RBC and Hb were at the control level, and Hct was increased compared with it as well as with the intact rats' values.

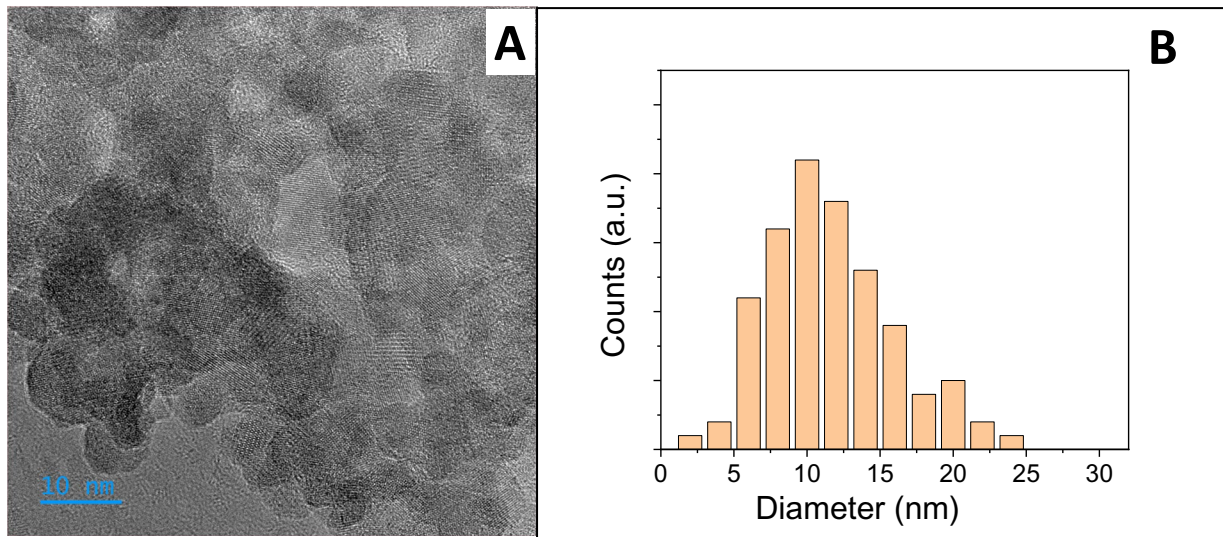


Fig. 3 TEM image (A) and size distribution (B) NPs in EB PVD 20 wt% Fe-NaCl condensate

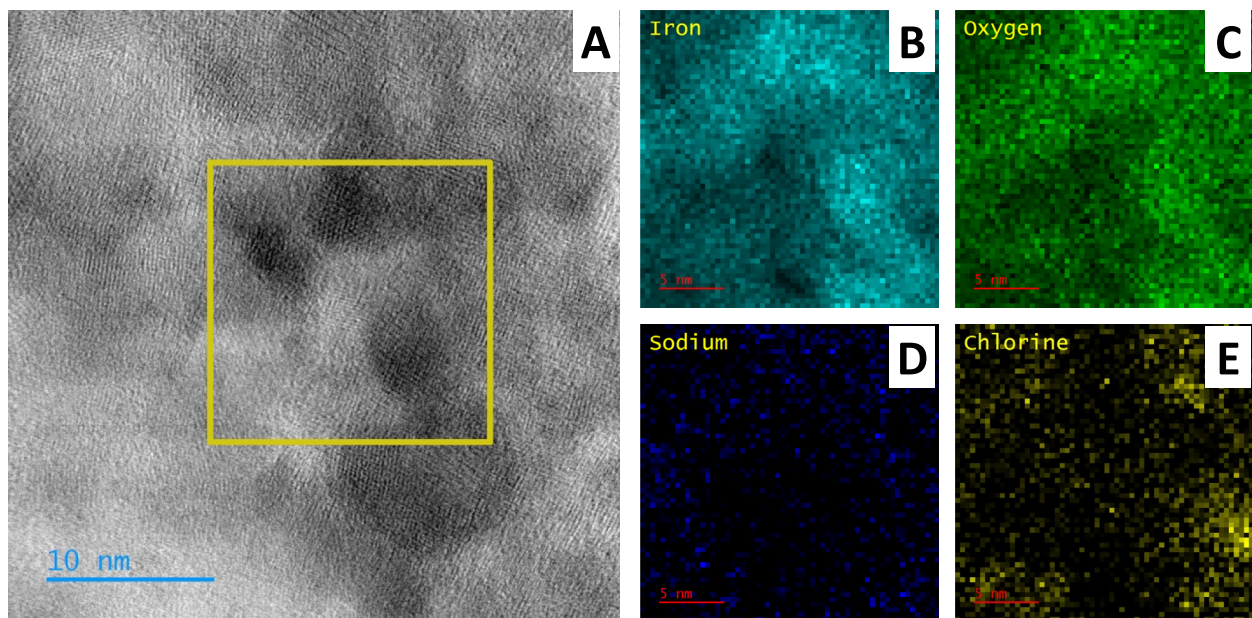


Fig. 4 STEM/HAADF image (A) and EDS mapping selected area iron (B), oxygen (C), sodium (D) and chlorine (E) of EB PVD 20 wt% Fe-NaCl condensate

The administration of the reference preparation Ferrum Lek to rats with a further study after 72 h caused an increase in the MCH ($p < 0.001$) and MCHC ($p < 0.001$) and a decrease in RDW ($p < 0.005$) in comparison with the animals of the control group. The MCV index in the reference group did not change. When $\text{Fe}_3\text{O}_4@\text{NaCl}$ NPs were used, only a decrease in RDW was observed 72 h after. The rest of the indices were at the level of the

control. The MCH and MCHC were significantly lower ($p < 0.001$) as compared to these indices under the reference preparation influence.

72 h after the administration of Ferrum Lek, the content of Rt in the blood of rats was 10.8% higher than that in the control, which, however, was not probable. In this period of observation, the content of Rt in animals with the $\text{Fe}_3\text{O}_4@\text{NaCl}$ NPs administration did not change compared to control.

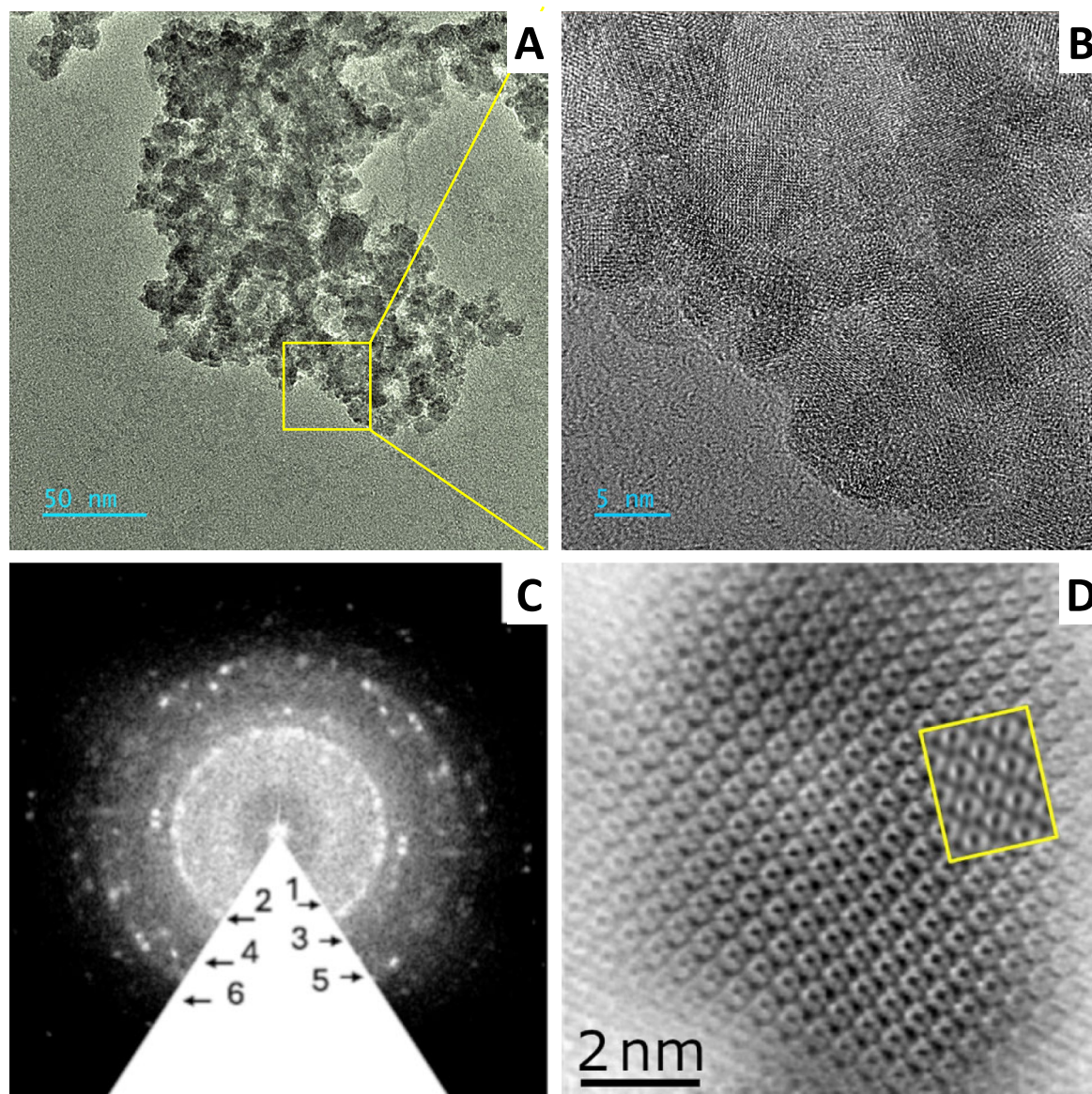


Fig. 5 TEM images (picture **A** and **B**), fast Fourier transform from image **B** (picture **C**) and STEM image (picture **D**) obtained from NPs in EB PVD 20 wt% Fe-NaCl condensate, the inset shows the simulated image

Therefore, the administration of NPs in the NaCl matrix to rats without any experimental pathology was characterized by a transient increase in the main indicators of red blood accompanied by an increase in the saturation of erythrocytes with hemoglobin and its mean volume that was stronger than the etalon iron drug effect after 3 h.

Blood gases, electrolytes and pH

3 h after the administration of saline solution to rats of the control group, $p\text{CO}_2$, $p\text{O}_2$, saO_2 and ctO_2 were at the level of intact animals' indicators (Table 5). All these

parameters did not change with the administration of reference preparation and NPs compared to control.

The blood pH was similar in all studied groups (Table 5). In rats with the Ferrum Lek use, there was a slight but probable decrease in the Na^+ concentration ($p < 0.05$) as compared to control. 3 h after the administration both of the NPs solution and reference preparation, the K^+ content in all groups did not change and stayed at the level of intact animals. The concentration of Ca^{2+} and standard bicarbonate also was unchanged.

72 h after the saline administration, $p\text{CO}_2$, $p\text{O}_2$, saO_2 , and ctO_2 did not change (Table 6). These indicators

Table 3 The effect of magnetite NPs in the NaCl matrix on hematological parameters 3 h after the administration to intact rats (M ± SEM)

Parameters	Groups of animals			
	Intact (n = 5)	Saline (n = 5)	Ferrum Lek (n = 5)	Fe ₃ O ₄ @NaCl (n = 6)
RBC, × 10 ¹² /L	6.94 ± 0.29	6.98 ± 0.29	6.95 ± 0.17	7.63 ± 0.24 ^{*,#^}
Hb, g/L	129.0 ± 3.3	128.2 ± 3.6	142.0 ± 2.6 ^{*,#}	145.3 ± 3.2 ^{*,#}
Hct, units	0.39 ± 0.01	0.40 ± 0.01	0.40 ± 0.01	0.46 ± 0.01 ^{*,#^}
MCV, μm ³	57.3 ± 0.9	57.4 ± 1.1	57.6 ± 0.5	61.0 ± 1.4 ^{*,#^}
MCH, pg	17.8 ± 0.4	17.7 ± 0.3	19.1 ± 0.4 ^{*,#}	20.4 ± 0.1 ^{*,#^}
MCHC, g/dL	317.2 ± 6.8	316.4 ± 7.7	355.2 ± 4.2 ^{*,#^}	313.8 ± 3.5 [^]
RDW, %	10.1 ± 0.3	10.0 ± 0.4	9.1 ± 0.2	9.7 ± 0.4
Rt, ‰	50.4 ± 4.0	50.6 ± 4.9	44.4 ± 6.7	45.5 ± 6.0

n is the number of animals in the group

Data are presented as mean and its standard error (M ± SEM)

* p < 0.05 as compared to intact animals

p < 0.05 as compared to saline (control)

^p < 0.05 as compared to Ferrum Lek, a reference drug

Table 4 The effect of magnetite NPs in the NaCl matrix on hematological parameters 72 h after the administration to intact rats (M ± SEM)

Parameters	Groups of animals			
	Intact (n = 5)	Saline (n = 5)	Ferrum Lek (n = 5)	Fe ₃ O ₄ @NaCl (n = 6)
RBC, × 10 ¹² /L	6.94 ± 0.29	6.95 ± 0.29	6.96 ± 0.16	7.71 ± 0.22
Hb, g/L	129.0 ± 3.3	128.8 ± 3.3	148.0 ± 2.5 ^{*,#}	139.8 ± 2.0
Hct, units	0.39 ± 0.01	0.39 ± 0.01	0.41 ± 0.01	0.45 ± 0.01 ^{*,#}
MCV, μm ³	57.3 ± 0.9	57.4 ± 1.0	58.7 ± 0.5	58.2 ± 0.7
MCH, pg	17.8 ± 0.4	17.6 ± 0.3	21.2 ± 0.3 ^{*,#}	18.1 ± 0.3 [^]
MCHC, g/dL	317.2 ± 6.8	317.4 ± 7.8	362.0 ± 2.4 ^{*,#}	312.2 ± 2.9 [^]
RDW, %	10.1 ± 0.3	10.0 ± 0.3	8.8 ± 0.3 ^{*,#}	8.6 ± 0.4 ^{*,#}
Rt, ‰	50.4 ± 4.0	48.8 ± 4.6	59.6 ± 4.1	47.2 ± 8.2

n is the number of animals in the group

Data are presented as mean and its standard error (M ± SEM)

* p < 0.05 as compared to intact animals

p < 0.05 as compared to saline (control)

^p < 0.05 as compared to Ferrum Lek, a reference drug

remained stable in animals with the administration of the reference drug and NPs. At this period, blood pH and electrolytes of the control rats did not change compared to those in intact animals. When the reference drug or NPs were administered, changes were registered only in the Na⁺ concentration which decreased as compared to control (p < 0.001).

Therefore, when administered to animals at the absence of any pathology, Fe₃O₄@NaCl NPs did not worsen blood gas parameters and pH and decreased only Na⁺ content in blood after 72 h that allows us not to worry about their

negative impact on such homeostatically important functions of the body as the transport of gases in the blood and acid–base balance.

Serum iron

It was shown that after 3 h, the iron content in the blood serum when saline solution was administered to control rats was the same as in intact animals (Fig. 6A). The use of Ferrum Lek increased this indicator by 1.7 times (p < 0.001) compared to control. Nanoparticles Fe₃O₄@NaCl also increased the iron content in blood serum

Table 5 The effect of magnetite NPs in the NaCl matrix on blood gases, pH and electrolytes 3 h after the administration to intact animals (M ± SEM)

Parameters	Groups of animals			
	Intact (n = 5)	Saline (n = 5)	Ferrum Lek (n = 5)	Fe ₃ O ₄ @NaCl (n = 6)
pCO ₂ , mm Hg	40.8 ± 1.0	40.9 ± 1.0	38.2 ± 1.8	40.1 ± 0.8
pO ₂ , mm Hg	72.0 ± 4.5	71.6 ± 3.8	65.0 ± 5.1	64.3 ± 5.6
saO ₂ , %	90.8 ± 1.5	90.8 ± 1.6	89.3 ± 3.7	88.4 ± 1.1
ctO ₂ , units	18.3 ± 0.9	18.3 ± 0.6	17.8 ± 0.7	17.5 ± 1.3
pH, units	7.34 ± 0.02	7.34 ± 0.02	7.40 ± 0.01	7.37 ± 0.04
Na ⁺ , μM/L	142.0 ± 0.4	142.0 ± 0.4	140.4 ± 0.6 ^{*,#}	141.6 ± 0.6
K ⁺ , μM/L	3.0 ± 0.2	3.1 ± 0.2	2.9 ± 0.1	3.1 ± 0.2
Ca ²⁺ , μM/L	1.02 ± 0.01	1.02 ± 0.01	0.98 ± 0.06	0.97 ± 0.03
HCO ₃ ⁻ , μM/L	24.2 ± 0.7	24.2 ± 0.7	23.7 ± 0.9	24.5 ± 1.0

n is the number of animals in the group

Data are presented as mean and its standard error (M ± SEM)

* p < 0.05 as compared to intact animals

p < 0.05 as compared to saline (control)

Table 6 The effect of magnetite NPs in the NaCl matrix on blood gases, pH and electrolytes 72 h after the administration to intact animals (M ± SEM)

Parameters	Groups of animals			
	Intact (n = 5)	Saline (n = 5)	Ferrum Lek (n = 5)	Fe ₃ O ₄ @NaCl (n = 6)
pCO ₂ , mm Hg	40.8 ± 1.0	41.3 ± 0.9	39.2 ± 4.8	45.4 ± 5.3
pO ₂ , mm Hg	72.0 ± 4.5	72.4 ± 3.4	65.8 ± 6.5	65.8 ± 3.6
saO ₂ , %	90.8 ± 1.5	91.4 ± 1.6	90.7 ± 2.7	90.4 ± 2.3
ctO ₂ , units	18.3 ± 0.9	18.5 ± 0.7	18.9 ± 0.6	17.8 ± 0.5
pH, units	7.34 ± 0.02	7.34 ± 0.02	7.39 ± 0.03	7.35 ± 0.04
Na ⁺ , μM/L	142.0 ± 0.4	142.2 ± 0.4	139.9 ± 0.4 ^{*,#}	140.2 ± 0.5 ^{*,#}
K ⁺ , μM/L	3.0 ± 0.2	3.1 ± 0.2	3.2 ± 0.1	3.0 ± 0.2
Ca ²⁺ , μM/L	1.02 ± 0.01	1.01 ± 0.01	1.01 ± 0.04	0.98 ± 0.04
HCO ₃ ⁻ , μM/L	24.2 ± 0.7	23.9 ± 0.8	23.3 ± 0.9	24.6 ± 1.3

n is the number of animals in the group

Data are presented as mean and its standard error (M ± SEM)

* p < 0.05 as compared to intact animals

p < 0.05 as compared to saline (control)

by 1.4 times (p < 0.005) compared to that in the control group, but under the NPs influence, the iron concentration was probably lower than under the Ferrum Lek action (p < 0.05).

After 3 h, the TIBC in animals of the control group did not differ from that in intact rats (Fig. 6B). The applied reference preparation and NPs did not cause significant changes in this indicator compared to control. In this period, transferrin saturation with iron ranged from 44.3 to 66.8% (Fig. 6C). It was the same

in intact animals and in rats of the control group. A 1.5-fold increase in this indicator was observed when Ferrum Lek has been injected (p < 0.001) and 1.3-fold elevation when Fe₃O₄@NaCl has been administered (p < 0.005) compared to control.

72 h after injections of the reference preparation and tested NPs, the changes of the iron concentration in the blood serum continued to be recorded (Fig. 7A). These indicators were practically the same in intact animals and in the control. After the Ferrum Lek use, the iron concentration increased by 1.6 times

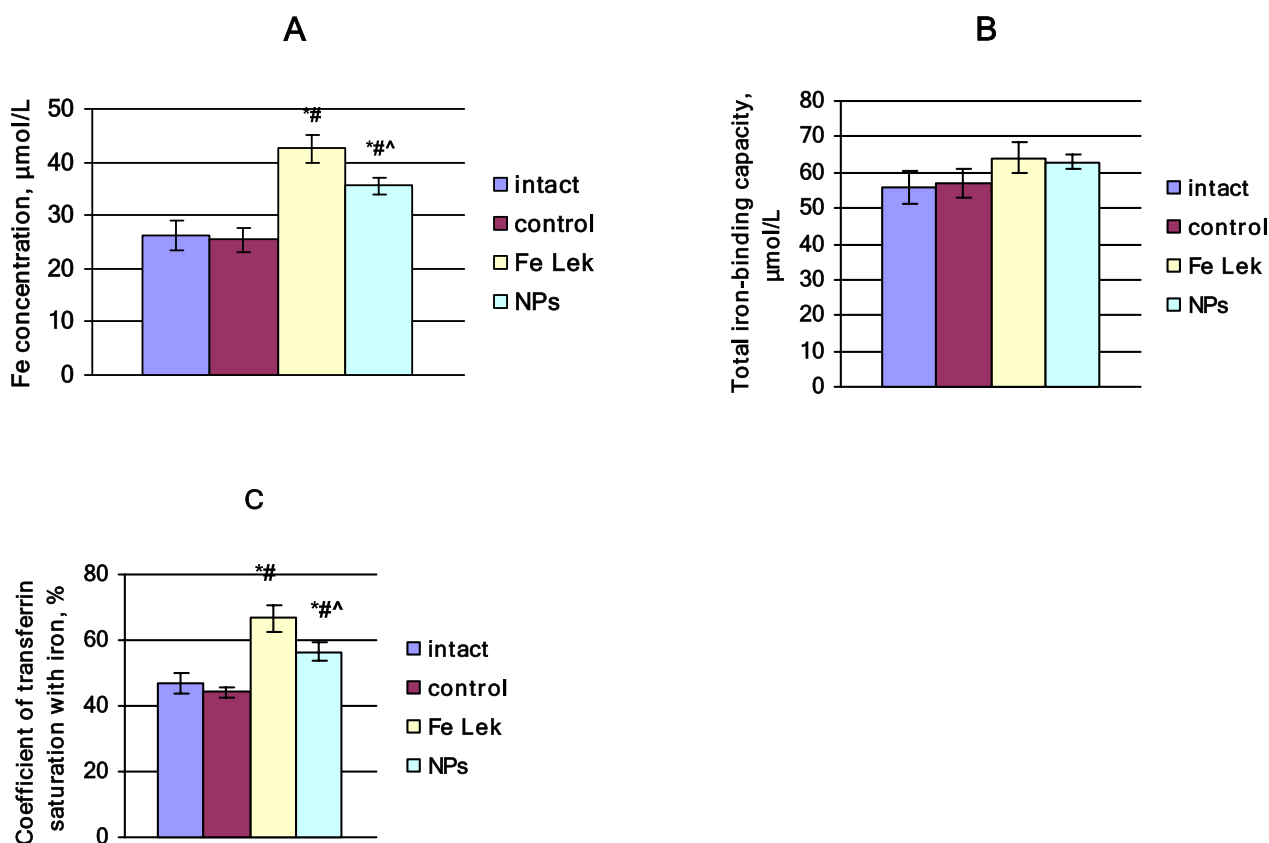


Fig. 6 The effect of magnetite NPs in the NaCl matrix on iron content (A), total iron-binding capacity (B) and transferrin saturation coefficient (C) in blood serum 3 h after the administration to intact animals. Data are presented as mean and its standard error ($M \pm \text{SEM}$). There were 5 animals in every group. * $p < 0.05$ as compared to intact animals, # $p < 0.05$ as compared to saline (control), ^ $p < 0.05$ as compared to the effect of Ferrum Lek. Abbreviations in the figure: Fe—iron, Fe Lek—Ferrum Lek, NPs—nanoparticles

($p < 0.005$) compared to control. When using $\text{Fe}_3\text{O}_4@$ NaCl, it elevated by 1.8 times ($p < 0.001$).

There were no changes in TIBC 72 h after the administration of the reference preparation and NPs (Fig. 7B). The saturation of transferrin with iron after 72 h was increased in comparison with the control both when Ferrum Lek was used and when the NPs solution was administered to animals (Fig. 7C). The degree of increase was 1.4 and 1.6 times, respectively, and the probability of these changes was $p < 0.001$ against control. The changes in these parameters were almost at the same level in the referent and experimental groups.

Therefore, $\text{Fe}_3\text{O}_4@$ NaCl NPs 3 h after the administration to rats cause an increase the iron content and saturation of transferrin in a less degree compared to the reference preparation; after 72 h, it acts similarly to etalon iron preparation.

Discussion

The use of HR TEM made it possible to study the obtained NPs in detail and identify them as pure (ligand-free) magnetite NPs. Evaporation by the EB PVD method through a molten liquid bath of pure iron and NaCl in vacuum and condensation of the mixed vapor streams on the substrate leads to crystallization of iron NPs in the NaCl matrix (Fig. 3A) with an average size of 11 nm and standard deviation of 5 nm (Fig. 3B). The absence of other impurities leads to obtaining the same NPs (Fig. 5A) with clean borders (Fig. 5B) and an ideal atomic structure inside the NPs (Fig. 5C, D). Extremely high chemical activity of synthesized iron NPs causes oxidation of iron NPs in air to magnetite (Fig. 1). All detected oxygen went to joining iron (Fig. 2) and forming magnetite (Tables 1, 2). Oxygen was not detected in the free status. This correlates with the element distribution map (Fig. 4B, C),

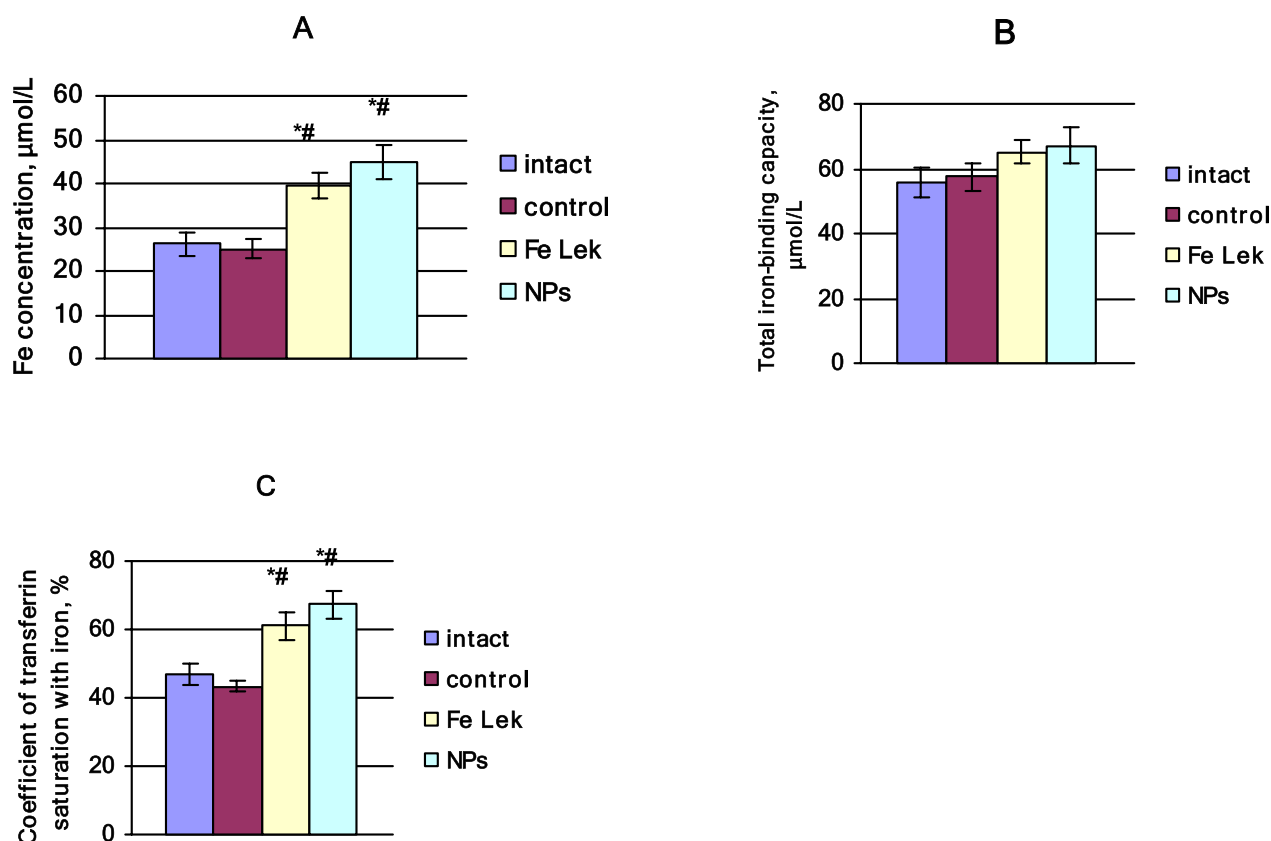


Fig. 7 The effect of magnetite NPs in the NaCl matrix on iron content (A), total iron-binding capacity (B) and transferrin saturation coefficient (C) in blood serum 72 h after the administration to intact animals. Data are presented as mean and its standard error ($M \pm \text{SEM}$). There were 5 animals in every group. * $p < 0.05$ as compared to intact animals, # $p < 0.05$ as compared to saline (control). Abbreviations in the figure: Fe—iron, Fe Lek—Ferrum Lek, NPs—nanoparticles

where the distribution of iron and oxygen completely coincides.

In contrast to previous works, where magnetite NPs with NaCl were used to correct posthemorrhagic syndrome, in this experiment their pharmacodynamics was monitored against the background of undisturbed homeostasis, which demonstrated significant differences in effects for the same dose and dosing regimen.

It was quite natural that the iron content in the blood serum increased 3 h after the administration of both the NP solution and the reference iron preparation Ferrum Lek. It was accompanied by an increase in transferrin saturation, which obviously reflects the participation of injected nano-iron in the normal transport and distribution of this element in the body [30]. At the same time, the TIBC of blood serum did not change, which can be explained by the normal balance of iron in the body, as it is known that this indicator increases under the conditions of iron deficiency [25].

It is known that magnetite NPs are in circulation for a short time and are quickly captured by cells of the

reticulo-endothelial system [31]. Obviously, after 3 h, we still find $\text{Fe}_3\text{O}_4@NaCl$ NPs in the circulatory system (even without additional coating with highly molecular weight agent), but the serum iron and transferrin saturation are lower than when using a traditional iron preparation, for which the plasma half-life is longer and is up to 30 h [30].

It can be assumed that under the conditions of this experiment, when there is no iron deficiency, in addition to the main way of incorporating iron into metabolic processes mediated by macrophages, the release of a significant amount of labile iron from NPs or a complex with carbohydrates is also important (although this is not characteristic of Ferrum Lek as a drug with a molecular weight of about 50 kD), which can lead to saturation of transferrin, and to the appearance of a significant amount of iron unbound to transferrin in blood plasma/serum [30] which was recorded by us.

Comparing serum iron levels with hematological parameters, it can be noted that magnetite NPs cause a stronger red blood reaction at lower serum iron levels 3 h after administration as compared to etalon iron drug,

that clearly indicates their higher and faster activity in relation to erythron.

Along with the increased concentration of iron in the blood serum, an increase in Hb, RBC and Hct was observed already 3 h after the NPs administration. At the same time, there was no significant increase in the content of Rt in the blood. This could not indicate the activation of bone marrow erythropoiesis. It remains to assume a rapid release of deposited erythrocytes and (or) rapid maturation of Rt in the circulation and enhanced saturation them by hemoglobin. The latter is evidently confirmed by the increase in MCH and MCV indices in animals that received an injection of NPs. At the time of study, similar changes in Hb and the MCHC and MCH indices were caused by the reference preparation (iron hydroxide (III) complex with polymaltosate molecules). This allows us to assume that both in the case of nano-iron and in the case of a conventional parenteral iron preparation, the mechanism of rapid action on erythrocytes and erythropoiesis in healthy animals is the same, but the rate of development of the effect may vary.

When determining blood gases, we did not find significant differences between the control and experimental groups, which can be explained by the balance of processes aimed at maintaining these vital functions in the body of healthy animals.

Testing of blood pH and electrolytes showed that changes due to the action of magnetite NPs and the reference preparation concerned only the Na^+ content. In the group of rats with the standard iron drug, a decrease in the content of Na^+ in the blood was observed after 3 and 72 h, and in the animals with the NPs administration, this phenomenon was recorded 72 h after the injection. Most likely, such changes were explained by the processes of erythropoiesis and changes in ion transport in the membranes of erythrocytes associated with their age. After all, it is known that in the cells of a widely used *in vitro* model of mouse erythropoiesis (Friend's erythroleukemia cells), a low level of Na^+ contributes to the completion of the erythroid cells differentiation [32]. The correlation of sodium content with the level of hemoglobin is also indicated by some other authors [33–35]. We cannot directly involve these data in the explanation of our own results, since they relate to plasma Na^+ , show a positive correlation and are characteristic to anemia, while we determined the content Na^+ in the blood, its decrease was noted with an increase in hemoglobin and was determined against the background of a normal iron balance in the animal's body. Therefore, it remains to assume that the detected decrease in the Na^+ concentration is a consequence of rapid activation of erythropoiesis and/or the appearance of young erythrocytes in the bloodstream. It is appropriate to mention that after acute blood loss

and the use of magnetite NPs or Ferrum Lek against its background, the processes had an opposite nature: post-hemorrhagic anemia was accompanied by a decrease in Na^+ , and the recovery of hematological parameters was characterized by an increase in this parameter [36].

The detected changes in hematological parameters and sodium content during a single administration of magnetite NPs in the NaCl matrix (1.35 mg Fe/kg) to intact animals were small and did not go beyond the confidence intervals of the norm [37] and, obviously, were not of a pathological nature. This allows us to think that one-time administration of these NPs for diagnostic or therapeutic purposes is quite acceptable. The increase in serum iron was greater in percentage terms than the changes in the parameters mentioned above, but it is believed that the short-term increase in serum iron due to the exogenous administration is not of decisive clinical importance from the point of view that the amount of iron in the blood serum is only a small part of the iron, which is transferred to the site of erythropoiesis and is not proportional to the peak concentration in blood serum [30].

Conclusions

The purity (ligand-free) of EB PVD synthesized magnetite NPs was comprehensively confirmed by modern high-precision HR TEM microscopy with a resolution of 68 pm with a double spherical aberration corrector with all possible attachments: TEM, STEM, EDS, EELS, SAED, FFT.

As we can see, the investigated magnetite NPs show biological activity in the body of laboratory animals with undisturbed homeostasis and do so in a similar mechanism to the modern preparation of parenteral iron – iron hydroxide (III) polyisomaltosate. They cause a rapid increase in the level of serum iron and an equally rapid but transient appearance in the circulation of erythrocytes with an increased volume and hemoglobin content, which, presumably, may be a consequence of the accelerated maturation of reticulocytes in the circulation and stimulation of hemoglobin synthesis in them. The elimination of most of the hematological effects of used NPs after 72 h distinguished their effect from that of the reference iron preparation and confirmed the peculiarities of the pharmacokinetics of iron oxides NPs without a polymer coating.

The conducted studies demonstrated the ability of pure magnetite NPs in the NaCl matrix to cause certain changes in a healthy body. More intense rapid effects on hematological parameters at lower serum iron levels apparently indicate greater activity of the studied NPs compared to the known reference iron preparation. All detected effects were not toxic in nature and were not

long-lasting due to numerous compensatory reactions. They can become a basis for the following investigation directed on the development of new nano-preparation for blood loss and acute post-hemorrhagic anemia.

Abbreviations

Ca ²⁺	Calcium ion(s)
CMOS	Complementary metal oxide semiconductor
ctO ₂	Volume concentration of oxygen
EB PVD	Electron beam physical vapor deposition
EDS	Energy-dispersive X-ray spectroscopy
EELS	Electron energy-loss spectroscopy
Fe ₃ O ₄	Magnetite, iron (II, III) oxide
FFT	Fast Fourier transform
HAADF	High-angle annular dark-field imaging
Hb	Total hemoglobin
HCO ₃ ⁻	Standard bicarbonate
Hct	Hematocrit
HR TEM	High-resolution transmission electron microscopy
K ⁺	Potassium ion(s)
M ± SEM	Mean and its standard error
MCH	Mean cell hemoglobin
MCHC	Mean cell hemoglobin concentration
MCV	Mean cell volume
Na ⁺	Sodium ion(s)
NP(s)	Nanoparticle(s)
pCO ₂	Partial pressure of carbon dioxide
pH	Hydrogen index
pO ₂	Partial pressure of oxygen
RBC	Red blood cell(s)
RDW	Red blood cell distribution width
SAED	Selected Area Electron Diffraction
saO ₂	Hemoglobin saturation by oxygen
SI	Spectrum imaging
STEM	Scanning transmission electron microscopy
TEM	Transmission electron microscopy
TIBC	Total iron-binding capacity

Supplementary Information

The online version contains supplementary material available at <https://doi.org/10.1186/s40486-024-00209-x>.

Additional file 1.

Acknowledgements

The authors acknowledge the CERIC-ERIC Consortium for the access to Transmission Electron Microscope 200 kV JEOL (Japan) JEM-ARM200F NEOARM Holographic Electron Microscopy at the University of Salento (Lecce, Italy) and financial support of proposal 20232024 "Holo-TEM of magnetic nanocomplexes Au-Fe₃O₄-DOXO for a more effective fight against cancer".

Author contributions

L.S.: Investigation, Formal analysis, Visualization, Writing—Review & Editing V.E.: Conceptualization, Methodology of biomedical experiments, Data Curation, Writing—Original Draft M.D.: Investigation, Visualization, Writing—Review & Editing K.Yu.: Supervision, Conceptualization, Project administration C.L.: Data Curation, Visualization R.R.: Investigation, Visualization C.G.G.: Formal analysis, Software S.O.: Investigation, Formal analysis N.Ya.: Formal analysis, Software.

Funding

This research did not receive any specific grant from funding agencies in the public, commercial, or not-for-profit sectors.

Availability data and materials

The data supporting this article have been included as part of the Supplementary Information.

Declarations

Consent for publication

Not required.

Competing interests

The authors declare no competing interests.

Author details

¹Laboratory of Electron Beam Nanotechnology of Inorganic Materials for Medicine, E. O. Paton Electric Welding Institute of the National Academy of Sciences of Ukraine, 11 Kazymyr Malevych Street, Kyiv 03150, Ukraine. ²Department of Pharmacology, Poltava State Medical University, 23 Shevchenko Street, Poltava 36011, Ukraine. ³Department of Mathematics and Physics "E. De Giorgi", University of Salento, Via Monteroni, 73100 Lecce, Italy. ⁴Faculty of Computer Science and Cybernetics, Taras Shevchenko National University of Kyiv, 4D Akademika Hlushkova Ave, Kyiv 03680, Ukraine.

Received: 26 July 2024 Accepted: 8 September 2024

Published online: 08 October 2024

References

- Amos-Taouta BM, Fakayode OJ, Songca SP, Oluwafemi OS (2020) Effect of synthetic conditions on the crystallinity, porosity and magnetic properties of gluconic acid capped iron oxide Nanoparticles. *Nano-Struct Nano-Objects*. <https://doi.org/10.1016/j.nanoso.2020.10048>
- Tran HV, Ngo NM, Medhi R, Srinoi P, Liu T, Rittikulstitchai S, Lee TR (2022) Multifunctional iron oxide magnetic nanoparticles for biomedical applications: a review. *Materials*. <https://doi.org/10.3390/ma15020503>
- Gorobets O, Gorobets S, Sharai I, Polyakova T, Zablotskii V (2023) Interaction of magnetic fields with biogenic magnetic nanoparticles on cell membranes: physiological consequences for organisms in health and disease. *Bioelectrochemistry* 151:108390. <https://doi.org/10.1016/j.bioelechem.2023.108390>
- Niculescu AG, Chircov C, Grumezescu AM (2022) Magnetite nanoparticles: synthesis methods – a comparative review. *Methods* 199:16–27. <https://doi.org/10.1016/j.ymeth.2021.04.018>
- Lu L, Zheng H, Li Y, Zhou Y, Fang B (2023) Ligand-free synthesis of noble metal nanocatalysts for electrocatalysis. *Chem Eng J* 451(2):138668. <https://doi.org/10.1016/j.cej.2022.138668>
- Kurapov YA, Litvin SE, Belyavina NN, Oranskaya EI, Romanenko SM, Stelmakh YA (2021) Synthesis of pure (ligandless) titanium nanoparticles by EB-PVD method. *J Nanopart Res*. <https://doi.org/10.1007/s11051-020-05110-3>
- Wu Y, Lu Z, Li Y, Yang J, Zhang X (2020) Surface modification of iron oxide-based magnetic nanoparticles for cerebral theranostics: application and prospect. *Nanomaterials* 10(8):1441. <https://doi.org/10.3390/nano10081441>
- Lytvyn S, Vazhnichaya E, Kurapov Y, Semaka O, Babijchuk L, Zubov P (2023) Cytotoxicity of magnetite nanoparticles deposited in sodium chloride matrix and their functionalized analogues in erythrocytes. *Open Nano* 11:100143. <https://doi.org/10.1016/j.onano.2023.100143>
- Lu CH, Hsiao JK (2022) Diagnostic and therapeutic roles of iron oxide nanoparticles in biomedicine. *Tzu Chi Med J* 35(1):11–17. https://doi.org/10.4103/tcmj.tcmj_65_22
- Avasthi A, Caro C, Pozo-Torres E, Leal MP, García-Martín ML (2020) Magnetic nanoparticles as MRI contrast agents. *Top Curr Chem* 378(3):40. <https://doi.org/10.1007/s41061-020-00302-w>
- Grauer O, Jaber M, Hess K, Weckesser M, Schwindt W, Maring S, Wölfer J, Stummer W (2019) Combined intracavitary thermotherapy with iron oxide nanoparticles and radiotherapy as local treatment modality in recurrent glioblastoma patients. *J Neurooncol* 141(1):83–94. <https://doi.org/10.1007/s11060-018-03005-x>
- Huang Y, Hsu JC, Koo H, Cormode DP (2022) Repurposing ferumoxytol: diagnostic and therapeutic applications of an FDA-approved nanoparticle. *Theranostics* 12(2):796–816. <https://doi.org/10.7150/thno.67375>
- Cardoso VF, Francesko A, Ribeiro C, Bañobre-López M, Martins P, Lanceros-Mendez S (2018) Advances in magnetic nanoparticles for biomedical

- applications. *Adv Healthcare Mater.* <https://doi.org/10.1002/adhm.201700845>
14. Wen W, Wu L, Chen Y, Qi X, Cao J, Zhang X, Ma W, Ge Y, Shen S (2020) Ultra-small Fe₃O₄ nanoparticles for nuclei targeting drug delivery and photothermal therapy. *J Drug Deliv Sci Technol* 58:101782. <https://doi.org/10.1016/j.jddst.2020.101782>
 15. Su C (2017) Environmental implications and applications of engineered nanoscale magnetite and its hybrid nanocomposites: a review of recent literature. *J Hazard Mater* 322:48–84. <https://doi.org/10.1016/j.jhazmat.2016.06.060>
 16. Ebrahiminezhad A, Taghizadeh SM, Ghasemi Y, Berenjian A (2020) Immobilization of cells by magnetic Nanoparticles. *Methods Mol Biol* 2100:427–435. https://doi.org/10.1007/978-1-0716-0215-7_29
 17. Nowak-Jary J, Machnicka B (2023) In vivo biodistribution and clearance of magnetic iron oxide nanoparticles for medical applications. *Int J Nanomed* 18:4067–4100. <https://doi.org/10.2147/ijn.s415063>
 18. Kurapov YA, Vazhnichaya EM, Litvin SE, Romanenko SM, Didikin GG, Devyatkina TA, Mokliak YV, Oranskaya EI (2019) Physical synthesis of iron oxide nanoparticles and their biological activity in vivo. *SN Appl Sci* 1(1):102. <https://doi.org/10.1007/s42452-018-0110-z>
 19. Vazhnichaya E, Lytvyn S, Kurapov Y, Semaka O, Lutsenko R, Chunikhin A (2023) The influence of pure (ligandless) magnetite nanoparticles functionalization on blood gases and electrolytes in acute blood loss. *Nanomedicine: nanotechnology. Biol Med* 50:102675. <https://doi.org/10.1016/j.nano.2023.102675>
 20. Parasuraman S, Raveendran R, Kesavan R (2010) Blood sample collection in small laboratory animals. *J Pharm Pharmacol* 1(2):87–93. <https://doi.org/10.4103/0976-500x.72350>
 21. Bailly Y, Duprat P (1990) Normal Blood Cell Values Rat. In: Ward JM, Mohr U, Hunt RD (eds) Hemopoietic system monographs on pathology of laboratory animals. Springer, Berlin, Heidelberg, pp 27–38
 22. Brecher G (1949) New methylene blue as a reticulocyte stain. *Am J Clin Pathol* 19(9):895. https://doi.org/10.1093/ajcp/19.9_ts.895
 23. Hasan A (2009) Handbook of blood gas/acid–base interpretation. Springer-Verlag, London
 24. Stookey LL (1970) Ferrozine—a new spectrophotometric reagent for iron. *Anal Chem* 42:779–781. <https://doi.org/10.1021/ac60289a016>
 25. Rifai N, Horvath AR, Wittwer C (2018) Tietz textbook of clinical chemistry and molecular diagnostics. Elsevier, St. Louis, Missouri, Amsterdam
 26. Ewels P, Sikora T, Serin V, Ewels CP, Lajaunie L (2016) A complete overhaul of the electron energy-loss spectroscopy and X-ray absorption spectroscopy database: Eelsdb.eu. *Microsc Microanal* 22(3):717–724. <https://doi.org/10.1017/S1431927616000179>
 27. Gloter A, Douiri A, Tencé M, Colliex C (2003) Improving energy resolution of EELS spectra: an alternative to the monochromator solution. *Ultra-microscopy* 96(3–4):385–400. [https://doi.org/10.1016/S0304-3991\(03\)00103-7](https://doi.org/10.1016/S0304-3991(03)00103-7)
 28. Gloter A, Zbinden M, Guyot F, Gaill F, Colliex C (2004) TEM-EELS study of natural ferrihydrite from geological-biological interactions in hydrothermal systems. *Earth Planetary Sci Let.* <https://doi.org/10.1016/j.epsl.2004.03.040>
 29. Fujii T, de Groot FMF, Sawatzky GA, Voogt FC, Hibma T, Okada K (1999) In situ xps analysis of various iron oxide films grown by (formula presented)-assisted molecular-beam epitaxy. *Phys Rev B: Condens Matter Mater Phys* 59(4):3195–3202. <https://doi.org/10.1103/PhysRevB.59.3195>
 30. Geisser P, Burckhardt S (2011) The pharmacokinetics and pharmacodynamics of iron preparations. *Pharmaceutics* 3(1):12–33. <https://doi.org/10.3390/pharmaceutics3010012>
 31. Nowak-Jary J, Machnicka B (2022) Pharmacokinetics of magnetic iron oxide nanoparticles for medical applications. *Journal of Nanobiotechnology* 20(1):305. <https://doi.org/10.1186/s12951-022-01510-w>
 32. Oliveira D, Nogueira-Pedro A, Santos E, Hastreiter A, Silva G, Borelli P, Fock R (2018) A review of select minerals influencing the haematopoietic process. *Nutr Res Rev* 31(2):267–280. <https://doi.org/10.1017/S0954422418000112>
 33. Koumpis E, Florentin M, Hatzimichael E, Liamis G (2020) Hyponatremia in patients with hematologic diseases. *J Clin Med* 9(11):3721. <https://doi.org/10.3390/jcm9113721>
 34. Mansoor F, Bai P, Kaur N, Sultan S, Sharma S, Dilip A, Kammawal Y, Shahid S, Rizwan A (2021) Evaluation of serum electrolyte levels in patients with anemia. *Cureus* 13(10):e18417. <https://doi.org/10.7759/cureus.18417>
 35. Patil S, Biradar SM, Holyachi R, Devarmani S, Reddy S (2023) Assessment of serum electrolytes and glycated hemoglobin level in non-diabetic iron-deficient anaemic patients. *Cureus* 15(5):e38656. <https://doi.org/10.7759/cureus.38656>
 36. Vazhnichaya EM, Lutsenko RV, Semaka OV, Deviatkina TO, Deviatkina NM, Kurapov YUA, Litvin SYE (2021) Blood gases and electrolytes under use of magnetite nanoparticles in blood loss. *World Med Biol* 3(77):194–198. <https://doi.org/10.26724/2079-8334-2021-3-77-194-198>
 37. Vigneshwar R, Arivalagan A, Mekala P, Imayarasi K (2021) Sex-specific reference intervals for Wistar albino rats: hematology and clinical biochemistry. *Indian J Ani Health* 60(1):58–65. <https://doi.org/10.36062/ijah.60.1.2021.58-65>

Publisher's Note

Springer Nature remains neutral with regard to jurisdictional claims in published maps and institutional affiliations.